

Broad-Band Balanced Duplexers*

CLARENCE W. JONES†

Summary—Balanced duplexer circuits are described and a comparison is made between the two principal configurations employing gaseous switching devices. The balanced tr duplexer is limited in power-handling ability, while the balanced atr duplexer has slightly greater received-signal insertion loss. An analysis is made of the reflecting properties of an atr array, and the practical upper limit of the number of array elements is determined.

A DUPLEXER, in the language of radar, is a switching device which disconnects the transmitter from the receiver, usually by means of gaseous discharge tubes called tr's and atr's. There are at least three principal types of duplexers, each of which may have several variations dependent upon the specific application, power level to be handled, or bandwidth required. These types are: 1) branching duplexer, 2) polarization-twist duplexer, and 3) balanced duplexer. This classification does not cover all of the possible configurations of duplexers which employ gaseous discharge switches, nor does it include the duplexers employing ferrite-switching elements, although a large percentage of these ferrite devices could be included under categories 2) and 3).

The bandwidth of a duplexer is determined by both the bandwidths of the switching tubes, tr's and atr's, and the circuit configuration. The branching duplexer is the simplest configuration but is not inherently broad band. Its performance near the band edges is greatly influenced by the transmitter impedance. Both the polarization-twist and the balanced-duplexer characteristics are unaffected by the transmitter impedance within the useful pass band. The balanced duplexer is inherently capable of the greatest bandwidth, in principle being limited only by the waveguide bandwidth.

Balanced duplexers can take on many physical shapes. They may be built in coaxial line with ring hybrids or quarter-wave coaxial hybrids,¹ in slab line using circuits equivalent to the coaxial circuits, or in waveguide with ring hybrids,² directional couplers, or magic tees.² The switching circuits may employ either narrow-band or broad-band tr and atr elements of waveguide or coaxial construction. It is also possible to mix the waveguide and coaxial construction if this has an advantage in a particular application.

* Original manuscript received by the PGMTT, April 2, 1956. The research in this document was supported jointly by the U. S. Army, Navy, and Air Force under contract with Mass. Inst. Tech., Cambridge, Mass.

† Lincoln Lab., M.I.T., Lexington, Mass.

¹ C. G. Montgomery, R. H. Dicke, and E. M. Purcell, M.I.T. Rad. Lab. Ser., McGraw-Hill Book Co., Inc., New York, N. Y., vol. 8, ch. 12, 1948.

² L. D. Smullin and C. G. Montgomery, "Microwave Duplexers," M.I.T. Rad. Lab. Ser., McGraw-Hill Book Co., Inc., New York, N. Y., vol. 14, ch. 8, 1948.

It is the purpose of this paper to analyze the operation of balanced duplexers, in particular the configurations employing directional coupler hybrid junctions. The analysis is best carried out through use of the scattering matrix.

SCATTERING MATRIX REPRESENTATION OF MICROWAVE CIRCUITS

The scattering matrix representation³ lends itself admirably to a large number of microwave problems, and will be used here in so far as practical to describe the behavior of balanced duplexers. The scattering matrix relates the waves traveling outward, at a set of n terminals to those waves traveling inward at the set of terminals. S will be used to designate a scattering matrix, with subscripts added where appropriate in order to avoid confusion. Thus we may write

$$\begin{bmatrix} E_{o1} \\ E_{o2} \\ \vdots \\ E_{on} \end{bmatrix} = \begin{bmatrix} S_{11} & S_{12} & \cdots & S_{1n} \\ \cdot & \cdot & \cdot & \cdot \\ \cdot & \cdot & \cdot & \cdot \\ S_{n1} & \cdot & \cdot & S_{nn} \end{bmatrix} \begin{bmatrix} E_{i1} \\ E_{i2} \\ \vdots \\ E_{in} \end{bmatrix} \quad (1)$$

The terms on the major diagonal, S_{11} , S_{22} , \cdots , etc., are the reflection coefficients that would be measured if all other terminals were terminated with a match. All other matrix elements are transfer terms, again applying to the case where the terminals are reflectionless.

In order to solve the duplexer problem represented by Fig. 1, it is necessary to obtain the scattering matrices for the switching elements and the hybrids. The switching element is a two-terminal device and can be represented by

$$S_s = \begin{bmatrix} S_{11} & S_{12} \\ S_{12} & S_{11} \end{bmatrix} \quad (2)$$

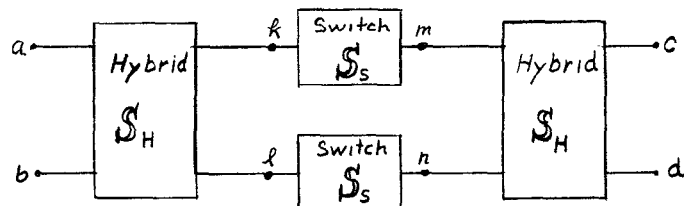


Fig. 1—Balanced duplexer.

The matrix is completely symmetrical because the reflection and transfer characteristics are the same when viewed from either terminal. The switch is a passive bi-

³ Montgomery, Dicke, and Purcell, *op. cit.*, ch. 5.

lateral device which has two operating conditions. S_{11} and S_{12} have two sets of values, one during the time the transmitter is on, and the other during the time the radar is receiving. More will be said about this in a later section.

The hybrid is a four-terminal device which ideally has the property that power supplied to a given terminal is equally divided between two of the three remaining terminals and nothing is coupled to the fourth terminal. It is possible to build hybrids which have a high degree of isolation and acceptable balance over a very wide band. For example, a multiple slot hybrid can have a directivity of 40 db and a deviation from 3 db coupling of 0.3 db over the 40 per cent waveguide band. If one properly numbers the terminals, the scattering matrix for an ideal directional coupler hybrid may be written

$$S_H = \frac{1}{\sqrt{2}} \begin{bmatrix} 0 & 0 & 1 & j \\ 0 & 0 & j & 1 \\ 1 & j & 0 & 0 \\ j & 1 & 0 & 0 \end{bmatrix}. \quad (3)$$

The term S_{12} is zero by definition for a perfect hybrid and so small in a practical unit that it can be set equal to zero without appreciable error. It can be proved⁴ that for $S_{12}=0$, $S_{11}=0$ also. In general the hybrids cannot be considered perfect, but for the case of the directional coupler hybrid, of either the multi-slot or the short-slot type, it has been found that calculations are sufficiently accurate if it is assumed that only the power split departs from ideal. The scattering matrix for this case may be written

$$S_H = \begin{bmatrix} 0 & \mathbf{H} \\ \mathbf{H} & 0 \end{bmatrix}, \quad (4)$$

where \mathbf{H} is a submatrix which contains the terms describing the power split. Eq. (4) applies to all types of hybrid circuits whose isolation is sufficiently good that S_{12} may be neglected. The form of \mathbf{H} is different for directional coupler hybrids than for magic tee and ring hybrids and, as a result, the circuit configurations vary with the type of hybrid or combinations of hybrids used. Fig. 2 illustrates this. The scattering matrix for ideal ring hybrids or magic tees (5) may be compared to the scattering matrix for the ideal directional-coupler hybrid (3).

$$S_T = \frac{1}{\sqrt{2}} \begin{bmatrix} 0 & 0 & 1 & 1 \\ 0 & 0 & -1 & 1 \\ 1 & -1 & 0 & 0 \\ 1 & 1 & 0 & 0 \end{bmatrix}. \quad (5)$$

The directional-coupler hybrid provides the duplexer circuit with the highest degree of symmetry, which would lead one to believe that this configuration should

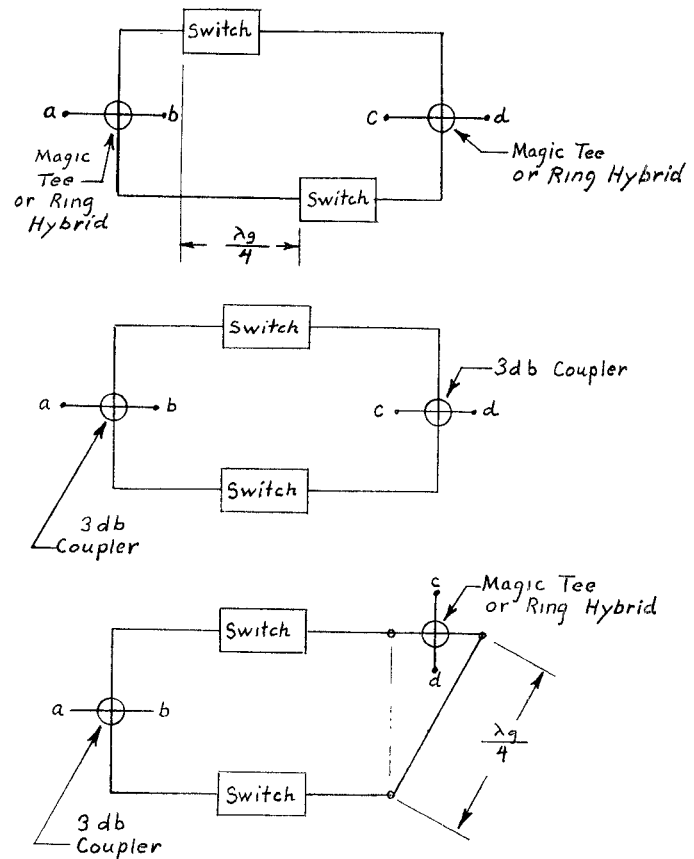


Fig. 2—Several possible balanced-duplexer configurations.

be capable of the greatest bandwidth. For purposes of this paper, only this type of duplexer will be considered from this point on.

BALANCED HYBRID DUPLEXER THEORY

Scattering Matrix of the Duplexer

Using nomenclature of Fig. 1, rearranging the scattering equations for identical switches, one can write

$$\begin{bmatrix} E_{0k} \\ E_{0l} \end{bmatrix} = S_{11} \begin{bmatrix} E_{ik} \\ E_{il} \end{bmatrix} + S_{12} \begin{bmatrix} E_{im} \\ E_{in} \end{bmatrix}. \quad (6)$$

The matrix equation for the duplexer then becomes

$$\begin{bmatrix} E_{0a} \\ E_{0b} \\ E_{0c} \\ E_{0d} \end{bmatrix} = \begin{bmatrix} S_{11} & \mathbf{H}^2 & S_{12} & \mathbf{H}^2 \\ S_{12} & \mathbf{H}^2 & S_{11} & \mathbf{H}^2 \end{bmatrix} \begin{bmatrix} E_{ia} \\ E_{ib} \\ E_{ic} \\ E_{id} \end{bmatrix}. \quad (7)$$

\mathbf{H} is the submatrix of (4) and may be written

$$\mathbf{H} = \begin{bmatrix} \sqrt{\frac{1+\alpha}{2}} & j\sqrt{\frac{1-\alpha}{2}} \\ j\sqrt{\frac{1-\alpha}{2}} & \sqrt{\frac{1+\alpha}{2}} \end{bmatrix}, \quad (8)$$

where α is a frequency-sensitive term governing the power split. Values of α by definition must lie in the range $-1 \leq \alpha \leq 1$.

⁴ *Ibid.*, ch. 9.

There are two principal types of balanced duplexers. The first employs balanced tr switches which reflect the transmitted power into the antenna. The second type employs balanced arrays of atr tubes which reflect the received signal into the receiver. These will be designated type I and type II respectively. The principal pieces of information desired are the relationships between the transmitter and antenna during the transmitting period and between the receiver and antenna during the receiving period. To determine this, it is necessary to reduce (7) to one involving only two of the four terminals. This can be done by terminating each of the other two terminals with a load having a reflection coefficient Γ . The two cases of interest are where 1) two terminals at the same end of the duplexer such as a and b of Fig. 1 are to be related, and 2) diagonally opposite terminals such as a and d are to be related.

After rearranging (7) and introducing the reflection coefficients Γ_c and Γ_d at the corresponding terminals, one may write the matrix equation

$$\begin{bmatrix} E_{0a} \\ E_{0b} \end{bmatrix} = \left(S_{11}P + S_{12}^2 \sum_{n=1}^{\infty} S_{11}^{n-1} (P\Gamma_1)^n P \right) \begin{bmatrix} E_{ia} \\ E_{ib} \end{bmatrix}, \quad (9)$$

where

$$P = H^2 = \begin{bmatrix} \alpha & j\sqrt{1-\alpha^2} \\ j\sqrt{1-\alpha^2} & \alpha \end{bmatrix} \quad (10)$$

$$\Gamma_1 = \begin{bmatrix} \Gamma_c & 0 \\ 0 & \Gamma_d \end{bmatrix}. \quad (11)$$

Relating a to d with b and c terminated gives

$$\begin{bmatrix} E_{0a} \\ E_{0d} \end{bmatrix} = \left(A + B \sum_{n=1}^{\infty} (\Gamma_2 A)^{n-1} \Gamma_2 B \right) \begin{bmatrix} E_{ia} \\ E_{ib} \end{bmatrix} \quad (12)$$

where

$$A = \begin{bmatrix} S_{11}P_{11} & S_{12}P_{12} \\ S_{12}P_{12} & S_{11}P_{11} \end{bmatrix} \quad (13)$$

$$B = \begin{bmatrix} S_{11}P_{12} & S_{12}P_{11} \\ S_{12}P_{11} & S_{11}P_{12} \end{bmatrix} \quad (14)$$

$$\Gamma_2 = \begin{bmatrix} \Gamma_b & 0 \\ 0 & \Gamma_c \end{bmatrix}. \quad (15)$$

Eqs. (9) and (12) describe the circuit characteristics of the two types of balanced duplexers being considered here. From them can be computed the vswr and insertion loss during both the transmitting and receiving phases. This is done by supplying the appropriate values of S_{11} and S_{12} , the switch tube parameters, which assume widely different values for the two operating conditions.

THE TRANSMITTING CONDITION

While the radar is transmitting, the tr and atr tubes will be ionized and may be represented by a short circuit. There is a finite voltage across these switches, but this

is, in any practical case, several orders of magnitude below the line voltage and may be ignored.

In the case of the type I duplexer the tr tubes place a short circuit across the transmission line so that $S_{11} = -1$ and $S_{12} = 0$. Substituting this into (9) gives

$$\begin{bmatrix} E_{0a} \\ E_{0b} \end{bmatrix} = -1 \begin{bmatrix} \alpha & j\sqrt{1-\alpha^2} \\ j\sqrt{1-\alpha^2} & \alpha \end{bmatrix} \begin{bmatrix} E_{ia} \\ E_{ib} \end{bmatrix}. \quad (16)$$

The vswr seen by the transmitter is

$$R_{T1} = \frac{1+\alpha}{1-\alpha} \quad (17)$$

and the insertion loss (neglecting the loss in the gas discharge) expressed in db is

$$L_{T1} = 10 \log \frac{1}{1-\alpha^2}. \quad (18)$$

For the type II duplexer where the atr windows are in the plane of the waveguide walls, the application of high power produces a discharge which shorts out these windows and the switch section appears like a piece of unperturbed transmission line except for the negligible voltage across the window. For this case $S_{11} = 0$ and $S_{12} = 1$. Substituting into (12) and expanding to $n = 1$

$$\begin{bmatrix} E_{0a} \\ E_{0b} \end{bmatrix} = \begin{bmatrix} \Gamma_c \alpha^2 & j\sqrt{1-\alpha^2} \\ j\sqrt{1-\alpha^2} & \Gamma_b \alpha^2 \end{bmatrix} \begin{bmatrix} E_{ia} \\ E_{ib} \end{bmatrix}. \quad (19)$$

Terms of order higher than $n = 1$ will be multiplied by the factor $\Gamma_b \Gamma_c$. Γ_b is arbitrary and is usually made to equal zero by connecting a matched load to terminal b . Terminal c is connected to the receiver, which will normally be protected by an auxiliary tr tube. This will provide a short circuit at terminal c so we may set $\Gamma_c = 1$.

The vswr becomes

$$R_{T2} = \frac{1+\alpha^2}{1-\alpha^2}. \quad (20)$$

The insertion loss is the same as for the type I duplexer. In this case the reflected power is absorbed in the termination at terminal b rather than being reflected back into the transmitter.

The dissipation in the switch tubes is not considered in (18) and is obviously so small as to have negligible effect on the circuit performance as seen at the terminals. However in a high power radar the switch tube dissipation is very important, since it is one of the principal power limiting factors. While it is not possible to calculate accurately the switch tube dissipation, it is possible to make a comparison between the power-handling capabilities of the two duplexer systems if it is assumed that the switch tube windows are identical. This is not an unrealistic situation and affords a good starting point when considering power handling capabilities.

At the output of the first hybrid the currents will be $1/\sqrt{2}I_0$, assuming perfect hybrid balance, where I_0 is the line current at the input terminal corresponding to a power P_0 . For the case of the type I duplexer, the tr tubes present a short circuit at which the current doubles. The window current is therefore $\sqrt{2}I_0$. If I_0 is the maximum current which the window can handle, then it is readily calculated that the line power must be reduced to $\frac{1}{2}P_0$. For the type II duplexer, the atr windows will be required to handle only $1/\sqrt{2}I_0$ and it is therefore possible to raise the transmitter power to $2P_0$ before the window capabilities are exceeded. All other things being equal, one would expect the atr type duplexer to handle four times the average power which can be switched by the tr type duplexer.

The transmitter load impedance is of importance in many applications. A comparison of (17) and (20), which are plotted in Fig. 3, shows that for the case of imperfect hybrids the atr duplexer has considerable advantage over the type I.

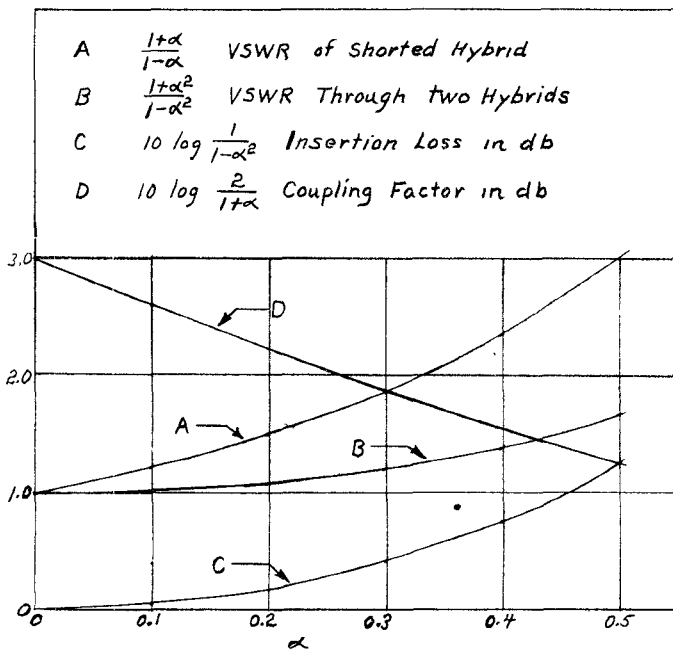


Fig. 3

THE RECEIVING CONDITION

During the receiving interval, only very weak signals enter the duplexer, so the insertion loss between the antenna and receiver is the only feature of interest. The receiving situation with the type I duplexer is described by (12), where terminals a and d are the antenna and receiver respectively. Γ_b is the reflection coefficient of the transmitter, and Γ_c that of the arbitrary load. The insertion loss expanded to $n = 1$ is

$$L_{R1} = 20 \log \left| \frac{1}{S_{12}\sqrt{1-\alpha^2} + S_{11}S_{12}\alpha\sqrt{1-\alpha^2}(\Gamma_b + \Gamma_c)} \right|. \quad (21)$$

Both S_{11} and α are normally small compared to unity within the useful pass band, so the second term in the denominator would ordinarily be neglected. S_{11} and S_{12} are the scattering coefficients for a particular tr switch.

The multiple-element broad-band tr tube is the switching element most used in the type I duplexer. This tube consists of several (usually two or three) quarter-wave-coupled resonant elements plus a low- Q window at each end which is also quarter-wave coupled to the other elements. There are a number of places in the literature where this type of band-pass filter is discussed.⁵⁻⁷ Fig. 4 shows the band-pass characteristic for a 1B58, from which values of S_{11} and S_{12} can be estimated.

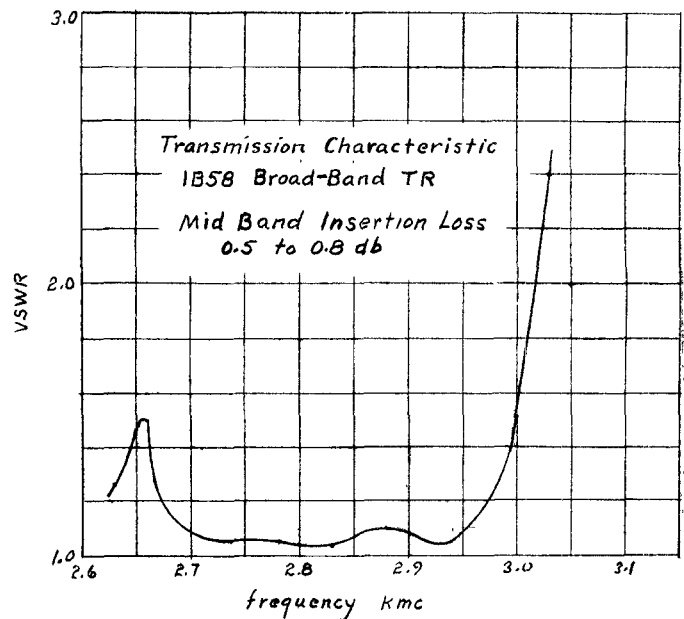


Fig. 4

During the receiving interval, the performance of the type II duplexer is described by (9). The switching circuit in this case is an array of one or more atr tubes. With the antenna at terminal a , the receiver at b , the transmitter having a reflection coefficient Γ_a at terminal d , and an arbitrary load of Γ_c at terminal c , the insertion loss expanded to $n = 1$ is

$$L_{R2} = 20 \log \left| \frac{1}{S_{11}\sqrt{1-\alpha^2} + S_{12}^2\alpha\sqrt{1-\alpha^2}(\Gamma_c + \Gamma_d)} \right|. \quad (22)$$

In this case S_{11} and S_{12} are the scattering terms for an atr array.

With the exception of those instances where one is interested in the duplexer behavior outside of the pass

⁵ W. L. Prichard, "Quarter wave coupled wave guide filters," *J. Appl. Phys.*, vol. 18, pp. 862-872; October, 1947.

⁶ G. L. Ragan, "Microwave Transmission Circuits," M.I.T. Rad. Lab. Ser., McGraw-Hill Book Co., Inc., New York, N. Y., vol. 9, p. 683, 1948.

⁷ Smullin and Montgomery, *op. cit.*, ch. 3.

band, the higher-order terms in the denominators of (21) and (22) can be ignored. In order to compare the performance of the two duplexers when receiving it is necessary to know the contributions to insertion loss made by the hybrids, the broad-band tr tubes, and the atr tube array. For type I

$$L_{R1} = 20 \log \left| \frac{1}{S_{12}} \right| + 20 \log \frac{1}{\sqrt{1 - \alpha^2}}, \quad (23)$$

where S_{12} is the transmission characteristic of the broad-band tr and α the balance factor of the hybrid. For type II, recalling that a broad-band tr is used in front of the receiver,

$$L_{R2} = 20 \log \left| \frac{1}{S_{11}} \right| + 20 \log \frac{1}{\sqrt{1 - \alpha^2}} + 20 \log \left| \frac{1}{S_{12}} \right|, \quad (24)$$

where S_{11} is the reflection factor of the atr tube array and S_{12} the transmission factor of the tr tube. All other things being equal it can be seen that the insertion loss of the atr duplexer is greater by the amount $20 \log |1/S_{11}|$.

THE ATR ARRAY

An atr tube is a shunt resonant circuit which is customarily mounted in series with the transmission line. An atr mounted on the broad surface of a rectangular waveguide is series mounted. When mounted on the narrow wall, the equivalent representation is a shunt circuit. The admittance matrix of the atr equivalent circuit, Fig. 5, is

$$Y = \begin{bmatrix} y & -y \\ -y & y \end{bmatrix} \quad (25)$$

where⁸

$$y = g + j2(1 + g)Q_L \frac{\Delta\omega}{\omega_0}. \quad (26)$$

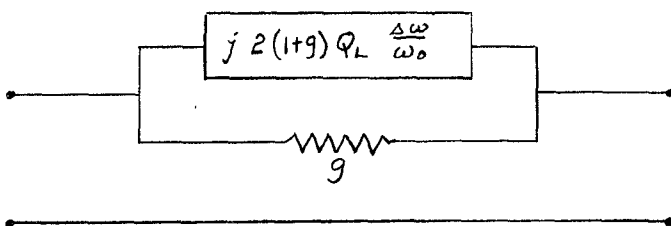


Fig. 5—Equivalent circuit of atr.

In order to compute the insertion loss of (22) it is necessary to obtain the scattering matrix for an array of tubes. This may be done by first obtaining the scattering

matrix for a single tube using the relation⁹

$$S = (1 - Y)(1 + Y)^{-1} \quad (27)$$

with the result that

$${}_1S = \frac{1}{1 + 2y} \begin{bmatrix} 1 & 2y \\ 2y & 1 \end{bmatrix}. \quad (28)$$

The second step is to cascade a line length θ with the atr circuit as shown in Fig. 6. This transformation¹⁰ results in

$$S_\theta = \begin{bmatrix} S_{11} & S_{12}e^{-j\theta} \\ S_{12}e^{-j\theta} & S_{11}e^{-j2\theta} \end{bmatrix}. \quad (29)$$

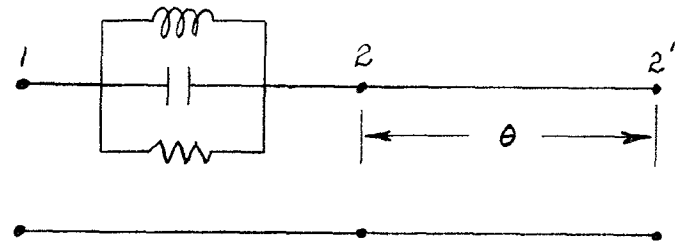


Fig. 6—Basic element of a tr array.

Except for the case where a line length is added at a terminal (29), the scattering matrix does not readily lend itself to cascading circuit elements. It is much more convenient at this point to transform to the T matrix^{11,12} which has the form

$$\begin{bmatrix} E_{02} \\ E_{i2} \end{bmatrix} = T \begin{bmatrix} E_{i1} \\ E_{01} \end{bmatrix}. \quad (30)$$

To cascade n elements it is only necessary to multiply the T matrices in reverse order

$${}_nT = T_n T_{n-1} \cdots T_1. \quad (31)$$

The transformations from the scattering matrix to the T matrix are

$$T = \begin{bmatrix} \left(S_{21} - \frac{S_{11}S_{22}}{S_{12}} \right) & \frac{S_{22}}{S_{12}} \\ -\frac{S_{11}}{S_{12}} & \frac{1}{S_{12}} \end{bmatrix} \quad (32a)$$

$$S = \begin{bmatrix} -\frac{T_{21}}{T_{22}} & \frac{1}{T_{22}} \\ \left(T_{11} - \frac{T_{12}T_{21}}{T_{22}} \right) & \frac{T_{12}}{T_{22}} \end{bmatrix}. \quad (32b)$$

The values of S_{11} for several arrays of identical atr tubes have been determined and are tabulated below.

⁹ Montgomery, Dicke, and Purcell, *op. cit.*, p. 148.

¹⁰ Montgomery, Dicke, and Purcell, *op. cit.*, p. 149.

¹¹ M. Tinkham and M. W. P. Strandberg, "The excitation of circular polarization in microwave cavities," *PROC. IRE*, vol. 43, pp. 734-738; June, 1955.

¹² Montgomery, Dicke, and Purcell, *op. cit.*, p. 150.

⁸ Smullin and Montgomery, *op. cit.*, p. 118.

$${}_1S_{11} = \frac{1}{1+2y} \quad (33a)$$

$${}_2S_{11} = \frac{\frac{1-4y^2}{1+2y} - (1+2y)e^{j2\theta}}{1 - (1+2y)^2 e^{j2\theta}} \quad (33b)$$

$${}_3S_{11} = \frac{\frac{1-4y^2}{(1+2y)^2} [(1-4y^2)e^{-j2\theta} - (1+2y)^2] - [1 - (1+2y)^2 e^{j2\theta}]}{\frac{1}{1+2y} [(1-4y^2)e^{-j2\theta} - (1+2y)^2] - (1+2y)[1 - (1+2y)^2 e^{j2\theta}]} \quad (33c)$$

$${}_4S_{11} = \frac{\frac{1-4y^2}{(1+2y)^3} [(1-4y^2)^2 e^{-j2\theta} - (3-4y^2)(1+2y)^2] + (1+2y)[3e^{j2\theta} - (1+2y)^2 e^{j4\theta}] - 4y^2(1+2y)e^{j2\theta}}{\frac{1}{(1+2y)^2} [(1-4y^2)^2 e^{-j2\theta} - (3-4y^2)(1+2y)^2] + (1+2y)^2 [3e^{j2\theta} - (1+2y)^2 e^{j4\theta}] + 4y^2} \quad (33d)$$

$${}_5S_{11} = \frac{\frac{1-4y^2}{(1+2y)^4} A - (1+2y)^2 B - 4y^2 [(3-4y^2)e^{j2\theta} - (1+2y)^2 e^{j4\theta}]}{\frac{1}{(1+2y)^3} A - (1+2y)^3 B + 4y^2 \frac{1-4y^2}{1+2y}} \quad (33e)$$

where

$$A = (1-4y^2)^3 e^{-j2\theta} - 4(1+2y)^2 (1-4y^2)(1-j^2)$$

$$B = 6 \frac{1-2y^2}{(1+2y)^2} e^{j2\theta} + 4e^{j4\theta} - (1+2y)^2 e^{j6\theta}.$$

Fig. 7 (next page) consists of several plots of $20 \log 1/S_{11}$. It can be demonstrated that half-wave spacing of identical atr tubes gives the widest pass band. Spacings different from half wave produce narrower pass bands or create "holes." Fig. 7(c), 7(d), 7(e), and 7(f) illustrates the effects of spacings different from half wave and indicate the spacing tolerance that must be held in order to maintain an acceptable pass band. An investigation of the effects of tuning errors in the atr circuits has not been attempted.

The curves of Fig. 7 have been plotted assuming an atr conductance of $g=0.02$. Several S-band tubes have been checked and it has been found that this is a realistic maximum figure. The resulting loss at band center is quite low, being less than 0.4 db for a single tube and less than 0.2 db for a three-tube array.

The 1-db insertion loss point has been arbitrarily chosen for bandwidth determination. The curve of Fig. 8 may be used for estimating bandwidth. This curve is a graphical determination from the data of Fig. 7 of the product BQ_L . It can be demonstrated that this product is very nearly constant for values of Q_L between three and ten. No attempt was made to obtain an explicit expression for $B=f(Q_L)$ because of the mathematical

complexity. Fig. 8 shows that there is nothing to be gained by constructing arrays of more than four elements. In practice it may develop that a three-element array is the largest practicable because of tuning tolerances and other circuit features which have not been taken into account in this treatment.

HYBRID CHARACTERISTICS

The short-slot hybrid¹³ is extensively used in balanced duplexer applications. Where balanced tr tubes are used the hybrid is customarily the side wall type, in which case the coupling is accomplished by means of an aperture in the common narrow wall of the waveguide. The top wall coupler which has two slots in the common broad dimension of the waveguide can also be used, and is a convenient configuration of the atr duplexer. Of the two types of short-slot hybrids, the top wall configuration has the best pass-band characteristic, but the side wall coupler will handle the most power. An attempt has been made by H. J. Riblet, originator of these types of hybrids, to increase the power handling ability of the top wall coupler by increasing the radii on the common wall. This has met with some success, but sufficient data are not available to make a valid comparison of the two types. Fig. 9 is a photograph of these two hybrid junctions. Fig. 10 (p. 12), shows values of α measured for a single model each of the side wall coupler and low-power

¹³ H. J. Riblet, "The short slot hybrid junction." PROC. IRE, vol. 40, pp. 180-184; February, 1952.

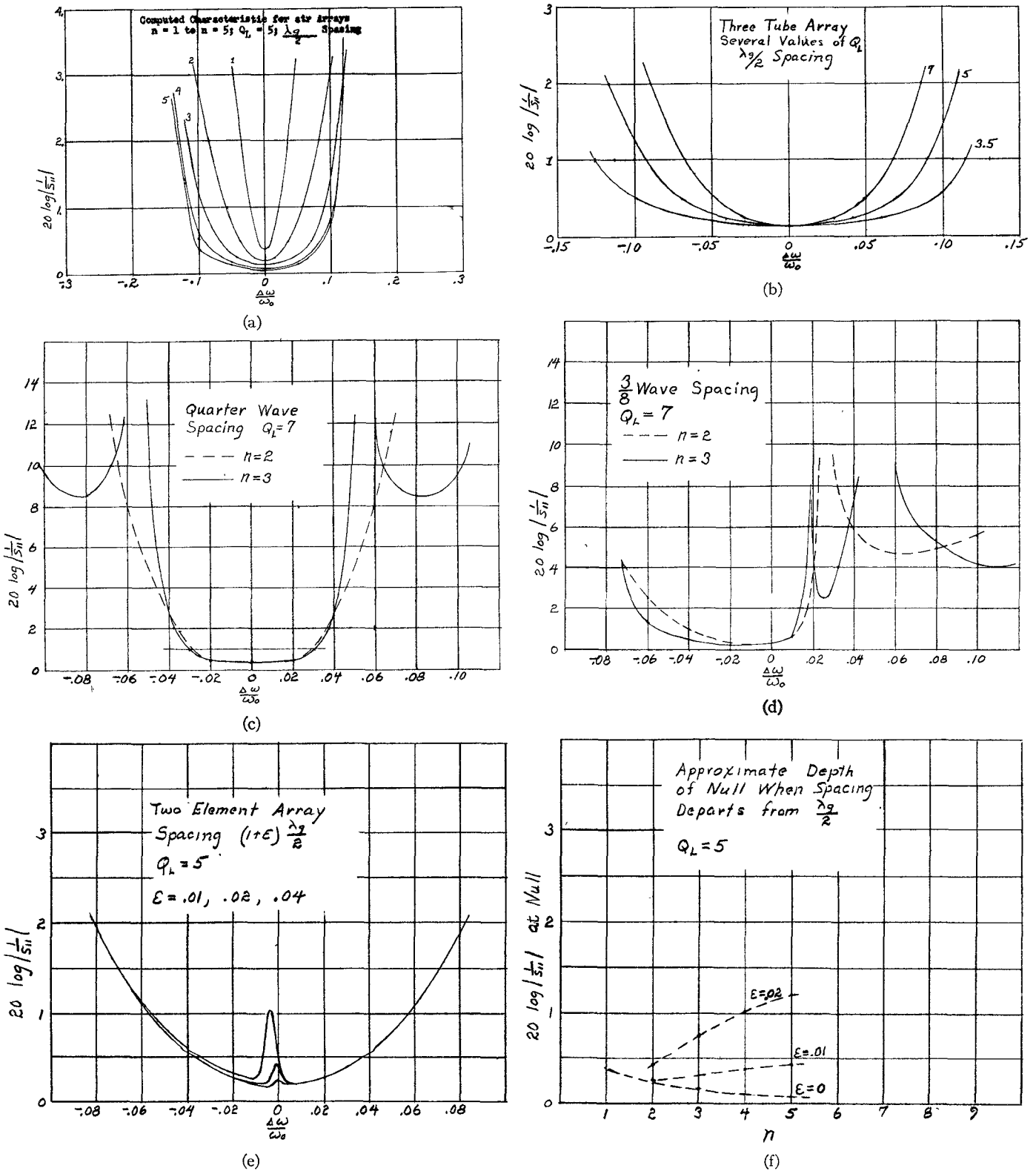


Fig. 7

top wall coupler, and the average of four models of the high power top wall coupler. In the latter case the units showed very little spread in characteristic over the band, 2600–3100 mc.

ATR TUBES

The choice of an atr tube array for the type II duplexer will be a compromise between bandwidth per

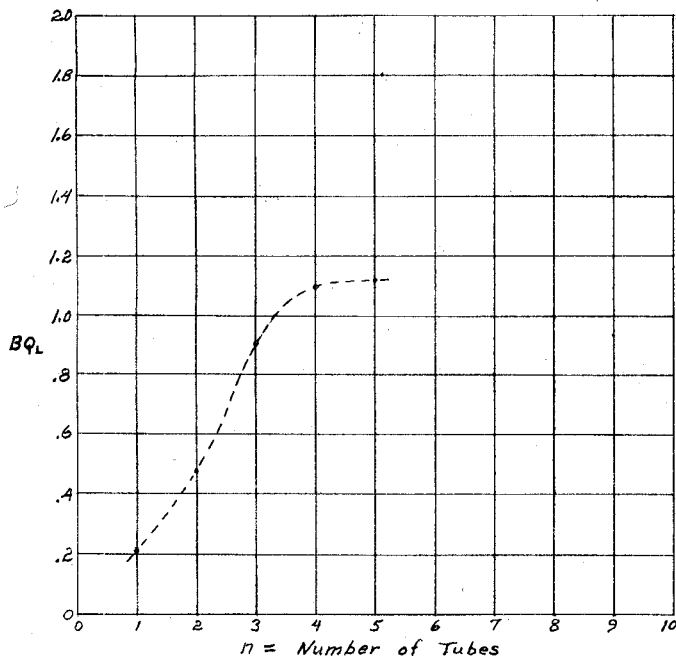


Fig. 8—Relationship between bandwidth ($B = \Delta\omega/\omega_0$ at 1 db) and number of half-wave spaced atr tubes.

Several S-band tubes have been procured from Bomac and Sylvania. Table I gives their low-level characteristics.

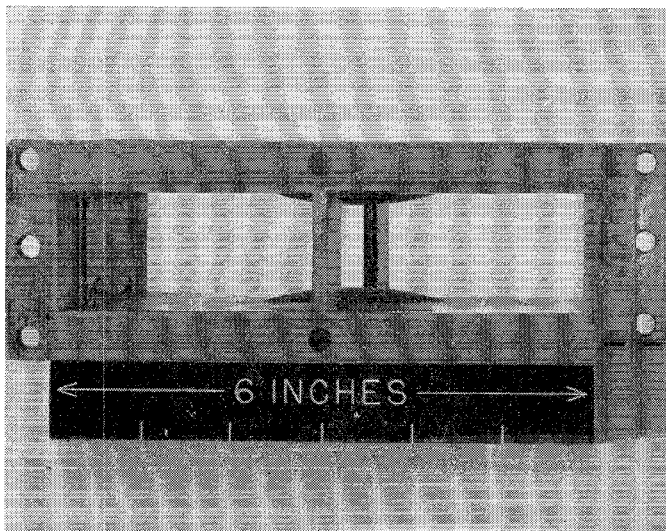
TABLE I*

Type	Q_L	mfr.
1B56	3.4	Bomac
1B56	3.3	Sylvania
BL623	5.5	Bomac
ATR788	5.5	Sylvania
BL632	9.4	Bomac

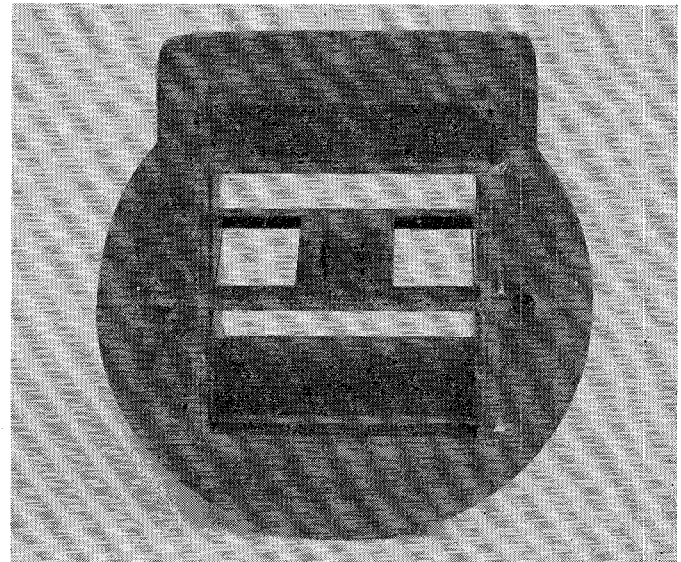
* $g \leq 0.02$ for all tubes.

EXPERIMENTAL S-BAND ATR DUPLEXER

Two atr duplexers were constructed, tested at low level, and then operated in radar systems in order to compare their performance with other existing duplexers. Unfortunately, the radars available did not have the transmitter power capabilities necessary for determining the useful upper limit of this type of duplexer. Some observations were made, however, which indicate that it is capable of handling high average power.



(a)



(b)

Fig. 9

tube and high level dissipation per tube. The higher the Q_L the greater the number of tubes required for a given bandwidth, but since the high- Q tubes have narrow windows, the arc voltage should be lower and one might expect the power lost per tube to be reduced. Sufficient data are not yet available regarding the relationship between dissipation and Q_L to form any conclusions at this point, but observations seem to confirm the suspicion that the dissipation goes at least as rapidly as $1/Q_L$ in the range $Q_L = 3.4$ to $Q_L = 9.4$.

The first of these duplexers employed two BL623 atr tubes (single-tube array) as the switching elements. The receiving bandwidth, which was that of the atr array, was 3.6 per cent. Bandwidth is arbitrarily defined as the per cent frequency between 1-db points of the atr array characteristic, *i.e.*, $L = 20 \log |1/S_{11}| = 1$. At 1.2 kw average power the switch tube temperature was about 140°F, as compared to a temperature in excess of 212°F for a 1B56 in a branching duplexer at the same power level. This is a crude comparison and should be

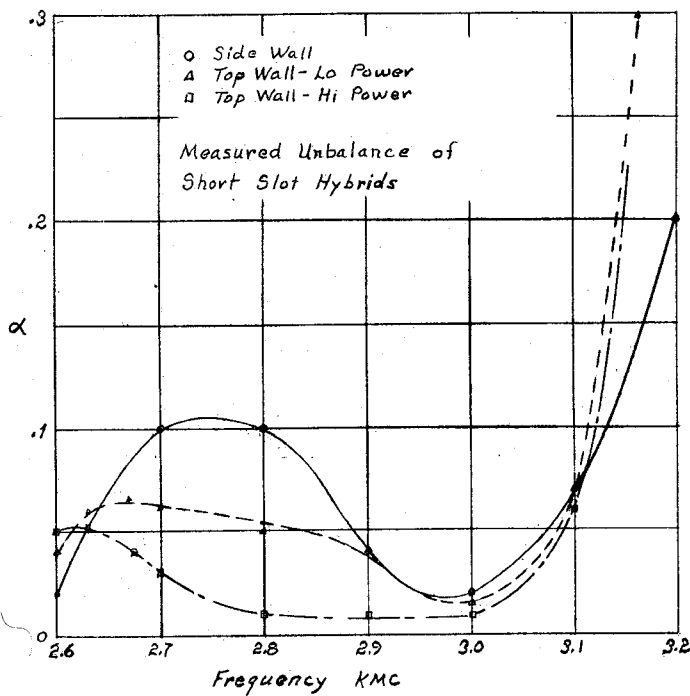


Fig. 10

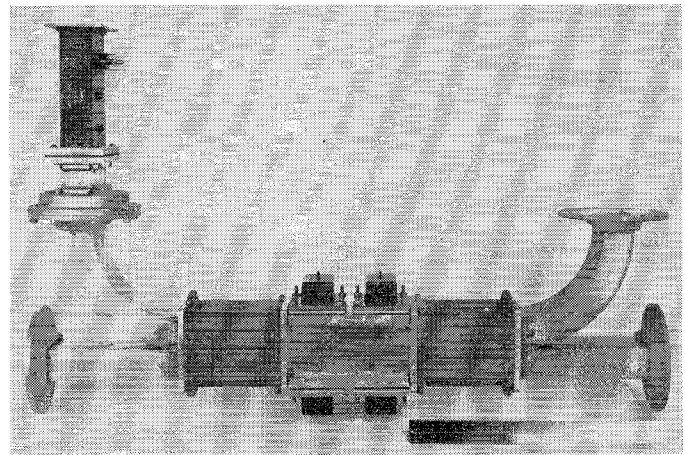


Fig. 11

considered only as a qualitative indication of the power handling ability.

The second duplexer, employing two-tube arrays in the switching circuit, behaved in a similar fashion at high level and had the predicted receiving bandwidth. This duplexer is shown in Fig. 11 (above).

Calculation of the Parameters of Ridge Waveguides*

TSUNG-SHAN CHEN†

Summary—In this paper an algebraic expression which constitutes an approximation to Cohn's transcendental equation is given for the determination of the dominant-mode cutoff wavelength of ridge waveguides. A modified derivation of Mihran's equation for calculating the characteristic impedance of ridge waveguides is discussed. Based upon these formulas, nomographs are constructed to permit the determination of these parameters with sufficient accuracy when the waveguide and the ridge dimensions vary. Experimental verification of the calculated cutoff wavelength is included.

INTRODUCTION

RIDGE WAVEGUIDES have a longer cutoff wavelength and a lower characteristic impedance than conventional rectangular waveguides having the same internal dimensions. The ridge waveguides also have a wider bandwidth free from higher-mode interference. Because of these advantages, ridge waveguides have been used as transmission links in systems requiring a wide free range in the fundamental mode,¹ as matching or transition elements in waveguide-to-

coaxial junctions,² as filter elements, and as components for other special purposes.³ One type of slow-wave structure used with traveling-wave tubes consists of a ridge waveguide which is made periodic by means of equally spaced transverse slots. The transverse resonant frequency of this structure corresponds to the cutoff frequency of the ridge waveguide.⁴

In the development of tunable magnetrons, double-ridge waveguides have been used as external tuning cavities because their reduced cutoff frequency permits a compact cavity section. Because the electric field is concentrated between the ridges, satisfactory tuning characteristics are obtained by means of a plunger which short-circuits the narrow gap. In the electron-beam method of frequency modulation, the beam is introduced in this region of strong electric field between two parallel plates attached to the ridges.

² Radio Res. Lab. Staff, Harvard Univ., "Very High-Frequency Techniques," vol. II, pp. 678-684, 731-736, McGraw-Hill Book Co., Inc., New York, N. Y.; 1947.

³ S. B. Cohn, "Properties of ridge waveguides," Proc. IRE, vol. 35, pp. 783-788; August, 1947.¹

⁴ J. R. Pierce, "Traveling-Wave Tubes," D. Van Nostrand Co., New York, N. Y., ch. 4; 1950.

* Manuscript received by PGMTT, March 14, 1956.

† Radio Corp. of America, Harrison, N. J.

¹ T. N. Anderson, "Double-ridge waveguide for commercial airlines weather radar installation," IRE TRANS., vol. MTT-3, pp. 2-9; July, 1955.